Parabolic quantum wells with the GaAs-$Al_xGa_{1-x}As$ system

R. C. Miller, A. C. Gossard, D. A. Kleinman, and O. Munteanu
AT&T Bell Laboratories, Murray Hill, New Jersey 07974
(Received 3 November 1983)

Photoluminescence measurements at 5 K on wafers containing parabolic quantum wells fabricated by molecular-beam epitaxy with the GaAs-$Al_{0.3}Ga_{0.7}As$ system reflect harmonic oscillator-like electron and hole levels. The many observed heavy-hole transitions can be fitted accurately with a model that divides the energy-gap discontinuity ΔE_g equally between the conduction and valence-band wells. This is in marked contrast to the usual $\Delta E_c = 0.85\Delta E_g$ and $\Delta E_v = 0.15\Delta E_g$ generally assumed for square wells. Experiment and theory show that parabolic wells can lead to parity-allowed $\Delta n = 2$ ("forbidden") transitions with strengths greater than that of nearby $\Delta n = 0$ ("allowed") transitions.

INTRODUCTION

It is well known that molecular-beam epitaxy (MBE) readily lends itself to the growth of structures requiring smooth and abrupt GaAs-$Al_xGa_{1-x}As$ heterointerfaces.[1,2] In addition, the MBE growth method is well suited to the fabrication of structures with various potential profiles, e.g., triangular quantum wells have been grown by MBE.[3] Recently, a pulsed Al source has been used with MBE to allow the growth of $Al_xGa_{1-x}As$ with an arbitrary Al profile.[4] This Rapid Communication describes the MBE growth and some of the characteristics of multiquantum well GaAs-$Al_xGa_{1-x}As$ structures with parabolic potential wells. As expected, these structures result in exciton transitions in the excitation spectra that reflect a uniformly spaced density-of-states function for the electrons and holes. The photoluminescence data also show enhanced "forbidden transitions,"[5,6] transitions with $\Delta n = 2$ but parity allowed. Analyses of the energies of the various exciton transitions suggest that the partitioning of the energy-gap discontinuities between the electron and valence-band wells may not be the same as that utilized for square wells.[7-9]

For square GaAs wells of width L_z and infinite height, the energy levels of a particle of mass m_i^* depend on L_z according to

$$E_{ni} = \frac{1}{2m_i^*}\left(\frac{n\pi\hbar}{L_z}\right)^2 , \tag{1}$$

where $n = 1, 2, 3$, etc. With parabolic wells

$$E_{ni} = (n - 1/2)\hbar\omega_{0i} , \tag{2}$$

where again $n = 1, 2, 3$, etc, and

$$\omega_{0i} = \sqrt{K_i/m_i^*} , \tag{3}$$

with K_i equal to the curvature of the parabolic well. Defining the curvature K_i by the potential height of the finite parabolic well at $z = \pm L_z/2$, namely, $Q_i\Delta E_g$, where ΔE_g is the total energy-gap discontinuity between the GaAs at the bottom of the wells and the $Al_xGa_{1-x}As$ at the top of the wells and Q_i is the fraction of ΔE_g for the ith particle well, Eq. (2) becomes

$$E_{ni} = 2(n - \tfrac{1}{2})\frac{\hbar}{L_z}\left(\frac{2Q_i\Delta E_g}{m_i^*}\right)^{1/2} . \tag{4}$$

It is interesting to note that the partitioning of the energy-gap discontinuity Q_i comes in directly in Eq. (4) but not in Eq. (1). Equations (1) and (4) are, of course, only approximations since the finite well heights should be taken into account as well as the dependence of the effective mass on the $Al_xGa_{1-x}As$ alloy composition x.

RESULTS

Parabolic compositional profiles were generated by alternate deposition of thin undoped layers of GaAs and $Al_xGa_{1-x}As$ of varying thickness. Computer control was employed in the deposition. The relative thicknesses of the $Al_xGa_{1-x}As$ layers increased quadratically with distance from the well centers while that of the GaAs layers decreased. Average layer thickness of approximately 10 Å were employed in order to permit the GaAs layers to be sufficiently thick to produce surface smoothing and cleaning,[10] while still allowing ample electron and hole tunneling to average the effective potentials to parabolic profiles. Each well contained 20 layers of $Al_xGa_{1-x}As$ and 21 layers of GaAs. The thickness of the Nth layer of $Al_xGa_{1-x}As$ from the center of the well was $[(N-0.5)/10]^2 \times L_z/20$. The $Al_xGa_{1-x}As$ layers are centered at distances $(N-0.5)L_z/20$ from the well center, and the remaining material is GaAs.

Figure 1 shows the photoluminescence and excitation spectra at 5 K from a parabolic well sample with ten periods where each period consists of a parabolic well estimated from the growth parameters to have $L_z = 510 \pm 35$ Å and barriers of width $L_B = 237 \pm 16$ Å composed of $x = 0.30 \pm 0.06$ alloy. The photoluminescence spectra were obtained with an excitation intensity $I_p = 0.14$ W/cm^2. The photoluminescence is relatively sharp, 2.2 meV full width at half maximum, and sufficiently intense to demonstrate that the Al-containing layers do not seriously degrade the recombination efficiency. The excitation spectrum with detection set at the photoluminescence peak exhibits much structure and shows essentially no Stokes shift between the $n = 1$ heavy-hole exciton E_{1h} and the emission peak. Thus, the main recombination from this sample is intrinsic and due to E_{1h} exciton emission as in the better quality square potential well samples.[11] Any electron density in the wells cannot exceed 5×10^{10} cm^{-2}.

Assignments of the various exciton transitions are also indicated in Fig. 1. Circular polarization excitation and detection techniques aided in the identification of some of the lower energy peaks.[5,11] The allowed transitions, $\Delta n = 0$, are identified by E_{nm}, where n is defined by Eq. (4) and m signi-

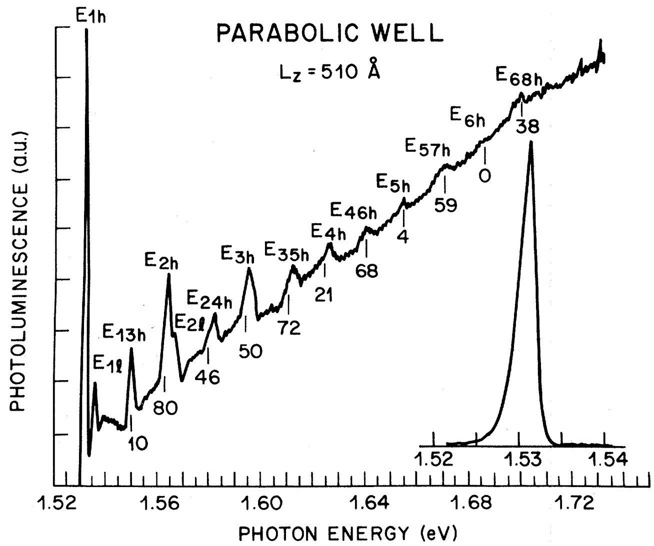

FIG. 1. The photoluminescence spectrum obtained at 5 K with 0.14 W/cm^2 excitation at 1.6 eV is shown in the insert. The excitation spectrum was taken with the same intensity as above and with the detection set at the peak of the photoluminescence, 1.531 eV. Various exciton transition peaks are labeled in the figure. Exciton transition energies for the heavy-hole excitons calculated using parabolic wells of equal height for the electrons and holes are shown as short vertical bars below the peaks. Their calculated strengths normalized to 100 for E_{1h} (without the resonant enhancement) are given as integers below the peaks. For $\Delta n \neq 0$, the sum of strengths of overlapping transitions, e.g., E_{24h} and E_{31h}, are included in the strength given.

fies whether the exciton transition involves a light or heavy hole, l or h, respectively. For the parity allowed "forbidden transitions,"[5,6] $\Delta n \neq 0$ but even, the designation $E_{nn'm}$ is used, where n refers to the electron level as above and n' the quantum number for the hole designated by m as above. Differences of the energies of the various transitions were then used to determine the energy-level ladders for electrons, heavy holes, and light holes, ΔE_e, ΔE_h, and ΔE_l, respectively. For these estimates, the binding energies of all the excitons were assumed equal.[12] The experimental values of ΔE_i are given in Table I along with estimates from Eq. (4) using the commonly accepted values for m_i^* and Q_i, namely, $m_e^*/m_0=0.0665$,[13] $m_h^*/m_0=0.45$,[13] $m_l^*/m_0=0.088$,[14] $Q_e=0.85$, and $Q_h=Q_l=1-Q_e=0.15$.[7] Data from two other parabolic well samples, $L_z=325\pm25$ Å and $L_z=336\pm25$ Å, are also given in Table I.

DISCUSSION

The agreement between the measured energy-ladder spacings and that calculated via Eq. (4) from the known growth parameters as given in Table I is poor. The L_z dependence of the calculated results can be removed by taking ratios of these energy ladders which then points up wherein the major problem lies. The average of the measured ratios are $\Delta E_e/\Delta E_h=2.6$, $\Delta E_e/\Delta E_l=1.4$, and $\Delta E_l/\Delta E_h=1.9$. These ratios are to be compared to calculated values; $\Delta E_e/\Delta E_h=6.0$, $\Delta E_e/\Delta E_l=2.7$, and $\Delta E_l/\Delta E_h=2.3$. The agreement between these two sets of numbers is also very poor except for $\Delta E_l/\Delta E_h$ and hence raises questions about the validity of Eq. (4) which assumes one effective mass throughout and parabolic wells of infinite height. With this in mind Eq. (4) was modified to include by perturbation theory the variation of the effective masses with z which results in a correction to the energy levels determined from Eq. (4) of

$$\delta E_i = -\frac{3.81\times10^3}{[L_z\ (\text{Å})]^2 m_i^*/m_0} f(m_i^*,x)(3-2n+2n^2)\ \text{meV}\ , \tag{5}$$

where for $x=0.3$, $f(m_i^*,x)=0.27$ for electrons and 0.17 for heavy holes. For the sample with $L_z=510$ Å this correction reduces the ladder spacings given in Table I by from 1.5% to 3.0% and hence for this L_z has little effect on the calculated ratios derived from Eq. (4). However, the correction to Eq. (4) given by Eq. (5) does result in calculated energy-level spacings that decrease slightly with increasing n as is usually

TABLE I. Experimental and calculated energy-level spacings for parabolic quantum wells.

	Expt.	Calc. Eq. (4)	"Exact" calc.
	$L_z=510\pm35$ Å, $x=0.30\pm0.06$		
ΔE_e (meV)	22.3	33.5	31.3
ΔE_h (meV)	8.4	5.4	5.2
ΔE_l (meV)	16.9	12.2	11.8
$\frac{\Delta E_e}{\Delta E_h}$	2.65	6.19	6.02
$\frac{\Delta E_e}{\Delta E_l}$	1.32	2.73	2.65
$\frac{\Delta E_l}{\Delta E_h}$	2.01	2.26	2.27
	$L_z=325\pm25$ Å, $x=0.29\pm0.06$		
ΔE_e (meV)	40.1	51.6	48.9
ΔE_h (meV)	15.6	8.33	8.1
ΔE_l (meV)	27.9	18.9	17.9
$\frac{\Delta E_e}{\Delta E_h}$	2.57	6.19	6.04
$\frac{\Delta E_e}{\Delta E_l}$	1.44	2.73	2.73
$\frac{\Delta E_l}{\Delta E_h}$	1.79	2.27	2.21
	$L_z=336\pm25$ Å, $x=0.30\pm0.06$		
ΔE_e (meV)	33.1	50.8	48.2
ΔE_h (meV)	12.4	8.20	8.0
ΔE_l (meV)	23.7	18.5	17.7
$\frac{\Delta E_e}{\Delta E_h}$	2.67	6.19	6.03
$\frac{\Delta E_e}{\Delta E_l}$	1.40	2.73	2.72
$\frac{\Delta E_l}{\Delta E_h}$	1.91	2.27	2.21

observed and predicted by the more exact calculation given below.

A better calculation of the energy levels has also been made using a program that determines the transmission of an arbitrary sequence of square-shaped wells and barriers as a function of energy. This computation includes any standing wave effects due to the discontinuous growth profile, the variation of the effective masses with x, the finite well height, and the boundary conditions for GaAs-$Al_xGa_{1-x}As$ interfaces proposed by one of us (D.A.K.) and independently by Bastard.[15] The results of these calculations are also given in Table I and they are found to differ by only a few percent from those determined from Eq. (4). The relatively good agreement between the experimental and calculated values of $\Delta E_l/\Delta E_h$ (15% $\pm$4%) suggests that the main difficulty involves the partitioning of the energy-gap discontinuity and not the hole masses. Since Eq. (4) gives results on ΔE_i that are only a few percent smaller than the values given by the better computation, Eq. (4) will be used to illustrate the problem with the partitioning of the energy-gap discontinuity. Equation (4) leads to

$$\frac{\Delta E_e}{\Delta E_h}=\left[\frac{Q_e}{1-Q_e}\frac{m_h^*}{m_e^*}\right]^{1/2}=2.6 \ , \tag{6}$$

which with the conventional masses m_i^* (Refs. 13 and 14) yields $Q_e \approx 0.50$. Thus there is a discrepancy when compared with the generally accepted value of $Q_e=0.85$ (Ref. 7) based on square-well spectra. However, there is some evidence that Q_e is sensitive to certain growth parameters.[16]

At present we have no explanation for the discrepancy between our value for Q_e and the accepted value. The parabolic wells we require to explain the observed ladder of levels could be produced by a combination of the accepted value $Q_e \approx 0.85$ and a negative space charge due to a density $n_{2D} \approx 1\times10^{12}$ cm^{-2} of either electrons or negatively charged acceptors. The absence of a Stokes shift between the emission peak and the $1h$ excitation peak rules out such a density of electrons in these samples. Also, with this density of electrons one would not see the $1h$ exciton peak in excitation at all. We believe the presence of such a density of acceptor or donor impurities is also ruled out by the fact that the same MBE apparatus produces quantum wells in modulation-doped samples exhibiting very high carrier mobilities. Therefore we believe space-charge effects in these samples are negligible.

Short vertical bars under the various peaks in Fig. 1 indicate energies of the heavy-hole transitions determined via the exact program using $Q_e=0.51$, $L_z=507$ Å, and $x=0.25$. Values of L_z and x employed are within the estimated uncertainties of these quantities given earlier. The calculation gives $\Delta E_e=22.8$ meV, $\Delta E_h=8.0$ meV, and $\Delta E_l=19.4$ meV. The calculated and experimental energies of the E_{1h} transition were set equal. The agreement between these calculated and experimental heavy-hole exciton transitions is considered excellent, but the L_z and x used are not unique. On the other hand, the calculated light-hole transitions (not shown) are too high in energy as expected since the calculated $\Delta E_l/\Delta E_h$ is too large.

One of the more striking characteristics of the data in Fig. 1 is the large strength of the "forbidden transitions" (parity allowed, $\Delta n=2$), especially those for large n. Strong forbidden transitions E_{13h} with resonant-type line shapes like that shown in Fig. 1 have been seen previously in multiquantum square-well structures.[17] For the undoped square-well case, theoretical estimates of the strengths of the forbidden transitions using finite square-well eigenfunctions which take into account different effective masses for the wells and barriers give values that are many orders of magnitude too small. These estimates have now been repeated using infinite parabolic-well eigenfunctions that include only GaAs masses. The calculated strengths (matrix elements squared) for E_{ijh} and E_{jih} are equal.[5,6] Also, since the spacing of the energy level ladder for the $\Delta n=0$ heavy-hole transitions is almost four times that of the heavy-hole ladder, transitions E_{24h} and E_{31h}, E_{35h} and E_{42h}, etc. are at nearly the same energy and hence are not expected to be resolved. Therefore to compare the calculated strengths with the excitation spectra, the strengths of overlapping transitions have been added together. The numbers under the various heavy-hole exciton transitions in Fig. 1 represent the integer values of the calculated strengths normalized to 100 for the calculated strength of E_{1h}. (The resonant enhancement of E_{1h} in Fig. 1 due to resonant Rayleigh scattering renders direct comparisons with this experimental peak meaningless.[18]) These results explain the large strengths of the $\Delta n\neq0$ transitions and the decreasing strength of the $\Delta n=0$ transitions as n increases. The strengths of these parity-allowed transitions arise from the fact that, in contrast to the square-well case, the hole and electron wave functions for parabolic wells have different spatial ranges for the same n, and for different n are not even approximately orthogonal. Thus, with parabolic wells, the $\Delta n\neq0$ parity-allowed transitions are not really "forbidden."

CONCLUSIONS

Photoluminescence spectra of GaAs-$Al_xGa_{1-x}As$ parabolic quantum-well samples reflect the expected harmonic oscillator levels. The observed level intervals suggest that the energy-gap discontinuity between the GaAs and $Al_xGa_{1-x}As$ layers is evenly split between the electron and valence-band wells. Theory and experiment show that the $\Delta n=2$ parity-allowed transitions are enhanced relative to the $\Delta n=0$ allowed transitions as n becomes large.

[1] C. Weisbuch, R. Dingle, A. C. Gossard, and W. Wiegmann, Solid State Commun. 38, 709 (1981).

[2] P. Petroff, A. C. Gossard, W. Wiegmann, and A. Savage, J. Cryst. Growth 44, 5 (1978).

[3] A. C. Gossard, W. Brown, C. L. Allyn, and W. Wiegmann, J. Vac. Sci. Technol. 20, 694 (1982).

[4] M. Kawabe, M. Kondo, N. Matsuura, and Kenya Yamamoto, Jpn. J. Appl. Phys. 22, L64 (1983).

[5] R. C. Miller, D. A. Kleinman, W. A. Nordland, Jr., and A. C. Gossard, Phys. Rev. B 22, 863 (1980).

[6] R. C. Miller, D. A. Kleinman, O. Munteanu, and W. T. Tsang, Appl. Phys. Lett. 39, 1 (1981).

[7] R. Dingle, Festkorperprobleme 15, 21 (1975).

[8] R. People, K. W. Wecht, K. Alavi, and A. Y. Cho, Appl. Phys. Lett. 43, 118 (1983).

[9] J. Sanchez-Dehesa and C. Tejedor, Phys. Rev. B 26, 5824 (1982).

[10]A. C. Gossard, W. Wiegmann, R. C. Miller, P. M. Petroff, and W. T. Tsang, in Proceedings of the 2nd International Conference on Molecular-Beam Epitaxy, Tokyo, 1982, p. 39 (unpublished). Also R. C. Miller, A. C. Gossard, and W. T. Tsang, Physica 117&118 B+C, Part II, 714 (1983).
[11]C. Weisbuch, R. C. Miller, R. Dingle, A. C. Gossard, and W. Wiegmann, Solid State Commun. 37, 219 (1981).
[12]R. C. Miller, D. A. Kleinman, W. T. Tsang, and A. C. Gossard, Phys. Rev. B 24, 1134 (1981).
[13]Q. H. F. Vrehen, J. Phys. Chem. Solids 29, 129 (1968).
[14]A. L. Mears and R. A. Stradling, J. Phys. C 4, L22 (1971).
[15]G. Bastard, Phys. Rev. B 24, 5693 (1981).
[16]See for example, R. S. Bauer and H. W. Sang, Jr., in *Surfaces and Interfaces: Physics and Electronics,* edited by R. S. Bauer (North-Holland, Amsterdam, 1983), p. 479.
[17]R. C. Miller (unpublished).
[18]J. Hegarty, M. D. Sturge, C. Weisbuch, A. C. Gossard, and W. Wiegmann, Phys. Rev. Lett. 49, 930 (1982).